

## Supporting information

# **Tumor acidity-responsive carrier-free nanodrug based on targeting activation *via* ICG-templated assembly for NIR-II imaging-guided photothermal-chemotherapy**

Kaihang Xue,<sup>†,a</sup> Feng Wei,<sup>†,c</sup> Jinyan Lin,<sup>\*,a,b</sup> Haina Tian,<sup>a</sup> Fukai Zhu,<sup>a</sup> Yang L.<sup>\*,d,e</sup>  
Zhenqing Hou<sup>a</sup>

<sup>a</sup>Department of Biomaterials, College of Materials, Research Center of Biomedical Engineering of Xiamen & Key Laboratory of Biomedical Engineering of Fujian Province, Xiamen University, Xiamen 361005, P. R. China

<sup>b</sup>The United Innovation of Mengchao Hepatobiliary Technology Key Laboratory of Fujian Province, Mengchao Hepatobiliary Hospital of Fujian Medical University, Fuzhou 350025, P. R. China

<sup>c</sup>Neurosurgical Department of Affiliated Zhongshan Hospital, Xiamen University, Xiamen 361004, P.R. China

<sup>d</sup>CAS Key Laboratory of Design and Assembly of Functional Nanostructures, Fujian Institute of Research on the Structure of Matter, Chinese Academy of Sciences, Fuzhou 350002, P.R. China

<sup>e</sup>Department of Translational Medicine, Xiamen Institute of Rare Earth Materials, Chinese Academy of Sciences, Xiamen 361024, P. R. China

\* Corresponding authors: Y. Li, liyang@xmu.edu.cn; J. Lin, linjinyan1988@163.com

<sup>†</sup>Author contributions: K. Xue and F. Wei contributed equally to this work.

## **Methods**

### **Materials**

Methotrexate (99%) and indocyanine green (97%) were obtained from Sigma-Aldrich Co., Ltd. (America). Dimethyl sulfoxide (DMSO) was received from Sinopharm Chemical Reagent Co., Ltd. (Shanghai, China). 3-(4, 5-dimethylthiazol-2-yl)-2, 5-diphenyltetrazolium bromide (MTT) was obtained from Sigma-Aldrich Co., Ltd (America). All other chemicals and solvents not mentioned were purchased from Sigma-Aldrich (St. Louis, MO) and used without further purification unless otherwise noted.

### **Characterization of IM**

The hydrodynamic diameter, polydispersity index (PDI), and zeta potential were measured by dynamic light scattering (DLS) and electrophoretic light scattering (ELS) using a Malvern Zetasizer 2000 (Malvern. U. K.), and the results were evaluated by mean  $\pm$  standard deviation (SD). The morphology was observed through transmission electron microscopy (TEM, JEM-2100, JEOL, Japan) operated at an accelerating voltage of 200 kV. The <sup>1</sup>H-NMR spectrum was performed on a Bruker AVANCE III 400MHz NMR spectrometer (Bruker, Germany) with DMSO-d<sub>6</sub> as solvents. The X-ray diffraction (XRD) pattern was performed on a Philips X'Pert Pro Super X-ray diffractometer (Philips, Netherlands). The Fourier Transform infrared (FT-IR) spectrum was performed on a Bruker IFS-55 infrared spectrometer (Bruker, Switzerland). The ultraviolet-visible-near-infrared (UV-vis-NIR) absorption spectrum was recorded with a Perkin Elmer Lambda 750 UV-vis-near-infrared spectrophotometer (Perkin-Elmer, USA). The fluorescence spectrum was recorded with a FluoroMax-4 Spectrofluorometer (HORIBA Jobin Yvon, USA).

### **Synthesis of PEG-CH=N-MTX (PEG-hyd-MTX)**

mPEG-CHO was synthesized between mPEG-OH and p-CBA under EDC/DMAP catalysis according to the previous literature. Afterward, PEG-CH=N-MTX (PEG-hyd-MTX) was synthesized between mPEG-CHO and aromatic amine of MTX via benzoic-imine linkage.<sup>32</sup> In brief, MTX (250 mg) was dissolved in 50 mL of dichloromethane/dimethylformamide (65/35, v/v). mPEG-CHO (500 mg) dissolved in dichloromethane was dropwise added to the above solution. After stirring at 40°C water bath under an argon atmosphere for 72 h, the organic solvent was concentrated by evaporation. The resultant was precipitated in an ice-cold ethyl ether, and then the crude precipitate was separated by decantation. After redissolving in dimethylformamide, the unreacted or excess MTX was removed from the resultant by filtration. The filtrate was evaporated, and then the product was redispersed in deionized water for dialysis (MWCO = 3500 Da) followed by lyophilization.

### ***In vitro* photothermal effect**

A fiber-coupled continuous semiconductor diode laser (808 nm, KS-810F-8000, Kai Site Electronic Technology Co., Ltd. China) was used in the experiments. ICG, IM, and P-hyd-IM were added into quartz cuvettes and irradiated by the 808 nm laser with a power density of 1 W/cm<sup>2</sup> for 5 min. The laser spot was adjusted to cover the entire surface of the sample. Real-time thermal imaging was performed and temperature change was monitored by a thermal infrared imaging camera (FLIR A5, FLIR Systems, USA).

### ***In vitro* PA imaging**

*In vitro* PA imaging and PA signal intensity of P-hyd-IM with different concentrations were obtained with an Endra Life Sciences Unveils Nexus 128 Photoacoustic Scanner (Ann Arbor, USA). The ICG and IM were used for comparison.

### ***In vitro* drug release**

*In vitro* release profiles of MTX from P-hyd-IM was determined by adding 2 mL of P-hyd-IM into a dialysis tube (molecular weight cut-off of 10, 000 Da) (Slide-A-

Lyzer, Thermo Scientific, USA), which was immersed into 60 mL of phosphate-buffered saline (PBS) at different pH values (7.4, 6.5 and 5.0). The release experiments were performed with/without 808 nm laser irradiation ( $1 \text{ W/cm}^2$ ) for 5 min at the time of initial experiment at  $37^\circ\text{C}$ . The mixture was then kept at  $37^\circ\text{C}$  in a shaker at 100 rpm. At predetermined time intervals, the dialysate was withdrawn followed by replacing with an equal volume of fresh PBS to continue further study. The release amount of MTX was measured by HPLC method as described above.

### ***In vitro* cellular uptake**

HeLa cells (human cervical carcinoma cell lines with overexpression of folate receptors), and A549 cells (human lung carcinoma cell lines with low expression of folate receptors) were seeded in 6-well plates at a density of  $1 \times 10^5$  cells per well. After 24 h of incubation, the cells were treated with ICG, ICG-FA, and IM at the same ICG concentration for different incubation time periods. Then, the cells were fixed with 4% paraformaldehyde for 15 min. Lastly, the cells were washed with cold PBS, stained with DAPI for 10 min, and examined by a Leica TCS SP5 confocal laser scanning microscopy (CLSM) (Leica Microsystems, Germany).

### ***In vitro* cytotoxicity assays**

HeLa cells were plated in 96-well plates in minimum essential media (DMEM) (10% fetal bovine serum and 1% penicillin), respectively. Cells were incubated at  $37^\circ\text{C}$  in a humidified atmosphere containing 5%  $\text{CO}_2$ . The medium was replaced with fresh medium after 24 h of culture. The drug formulations were diluted using cell culture medium to predetermined concentrations. For each well plate, 100  $\mu\text{L}$  of cell culture medium with different drug concentrations were added. Negative controls were created by addition of 100  $\mu\text{L}$  of culture medium. After 6 h of incubation, the medium was replaced with fresh medium and the cells were irradiated by 808 nm laser for 5 min at  $0.75 \text{ W/cm}^2$ . After laser irradiation, these cells were further incubated for another 18 h. After incubation, the medium was replaced with 100  $\mu\text{L}$  of medium containing 0.5 mg/mL of 3-(4, 5-dimethylthiazol-2-yl)-2, 5-diphenyltetrazolium

(MTT) and incubated with for 4 h. After removal of medium containing unreacted MTT, the left blue formazan crystals were dissolved in 100  $\mu$ L of DMSO, and the absorbance was measured in a BioTek Synergy H4 hybrid reader at a wavelength of 570 nm.

### ***In vitro* apoptosis assay**

Apoptosis of HeLa cells was detected using the Annexin V-FITC Apoptosis Detection Kit (BD Biosciences). The cells ( $1.0 \times 10^5$  cells per well) were seeded in 6-well plates. After culture for 48 h, the cells were respectively treated with ICG, MTX, IM, P-IM (pH 6.5) and P-hyd-IM (pH 6.5). After 6 h of incubation, the medium was replaced with fresh medium and the cells were irradiated by 808 nm laser for 5 min at  $0.75 \text{ W/cm}^2$ . After laser irradiation, these cells were further incubated for another 18 h. The subsequent procedures were performed according to the manufacturer's suggested procedures. The cells were analyzed by flow cytometry (FACSCalibur, BD Biosciences, USA) and CellQuest/FlowJo (Tree Star, USA) software.

### ***In vivo* NIR-II fluorescence and PA imaging**

To establish the HeLa breast tumor model,  $1 \times 10^6$  HeLa cells suspended in 40  $\mu$ L of PBS were subcutaneously inoculated into the flank region of each BALB/c nude mice. When the tumors reached to 100~200  $\text{mm}^3$ , the mice were randomly divided into four groups ( $n = 4$ ) and intravenously injected with ICG, IM, P-IM, and P-hyd-IM at equivalent ICG concentration (100  $\mu\text{g/mL}$ ) *via* the tail vein. *In vivo* NIR-II fluorescence images were obtained on Series II 900/1700 NIR-II small animal fluorescence imaging system (China) at 6, 12, and 24 h post-injection. The mice were euthanized at 24 h post-injection. The tumors as well as major organs (heart, liver, spleen, lung, and kidney) were harvested and then washed with cold saline for *ex vivo* NIR-II fluorescence imaging and semiquantitative biodistribution analysis using Series II 900/1700 NIR-II small animal fluorescence imaging system (China). *In vivo* PA signals were obtained on Endra Life Sciences Unveils Nexus 128 Photoacoustic Scanner (Ann Arbor, USA) at 6, 12, and 24 h of post-injection.

### ***In vivo* infrared thermal imaging**

HeLa breast tumor-bearing BALB/c nude mice were inoculated subcutaneously with  $1 \times 10^6$  HeLa cells in the flank region. When tumor volume approached  $\sim 120 \text{ mm}^3$ , the mice were randomly divided into five groups ( $n = 4$ ) and used for infrared thermal imaging. The tumor-bearing nude mice were *i. v.* injected with 200  $\mu\text{L}$  of PBS, ICG, IM, P-IM, and P-hyd-IM at equivalent concentration of ICG (1 mg/kg), respectively. At 12 h post-injection, the mice were anaesthetized by pentobarbital (0.5%) at a dosage of 45 mg/kg and the tumor sites were exposure to the 808 nm laser irradiation ( $1 \text{ W/cm}^2$ ) for 8 min. During laser irradiation, the temperature of tumors was monitored using thermal infrared imaging camera.

### ***In vivo* anticancer effect**

HeLa breast tumor-bearing BALB/c nude mice were prepared by subcutaneously injecting  $1 \times 10^6$  HeLa cells into the flank region. When the tumors reached to  $\sim 100 \text{ mm}^3$ , the mice were randomly divided into six groups ( $n= 6$ ): (i) PBS group; (ii) ICG plus laser irradiation group; (iii) IM plus laser irradiation group; (iv) P-IM plus laser irradiation group; (v) P-hyd-IM group; (vi) P-hyd-IM plus laser irradiation group. Then, the tumor sites in group (ii), (iii), (iv), and (vi) were irradiated by with 808 nm laser for 8 min after 12 h post-injection. The tumor volume and body weight were recorded every 3 days during the following 24 days. At the 24th day, the mice were euthanized, and the tumor as well as the main organs were excised, weighed, washed with 0.9% NaCl thrice, and fixed in the 10% neutral buffered formalin. For the hematoxylin and eosin (H&E) staining, the formalin-fixed tumors and main organs were embedded in paraffin blocks, sectioned at 8  $\mu\text{m}$ , stained with H&E, and examined by optical microscope (DM5500B, Leica Microsystems, Germany).

### **Hemolysis assay**

The red blood cells (RBCs) were isolated from serum by centrifugation of the mixture containing 0.5 mL of blood sample and 1 mL of PBS solution at 4, 500 rpm for 5 min. PBS was used to wash the RBCs five times and dilute the purified cells to 5 mL. Then

a certain volume of diluted RBCs suspension was added to quadruple volume of PBS solution with different concentrations of P-hyd-IM. The mixtures were vortexed and kept to stand for 3 h. Samples were then centrifuged to measure the absorbance of the supernatants at 541 nm by an UV-vis spectroscopy. RBCs treated with deionized water and PBS were set as positive and negative controls.

### **Statistical analysis**

Statistical significance was performed by using the t-test and one-way and two-way analyses of variance, in which  $P$  value  $< 0.05$  (\*) was considered significant,  $P < 0.01$  (\*\*) was very significant, and  $P < 0.001$  (\*\*\*) was highly significant.

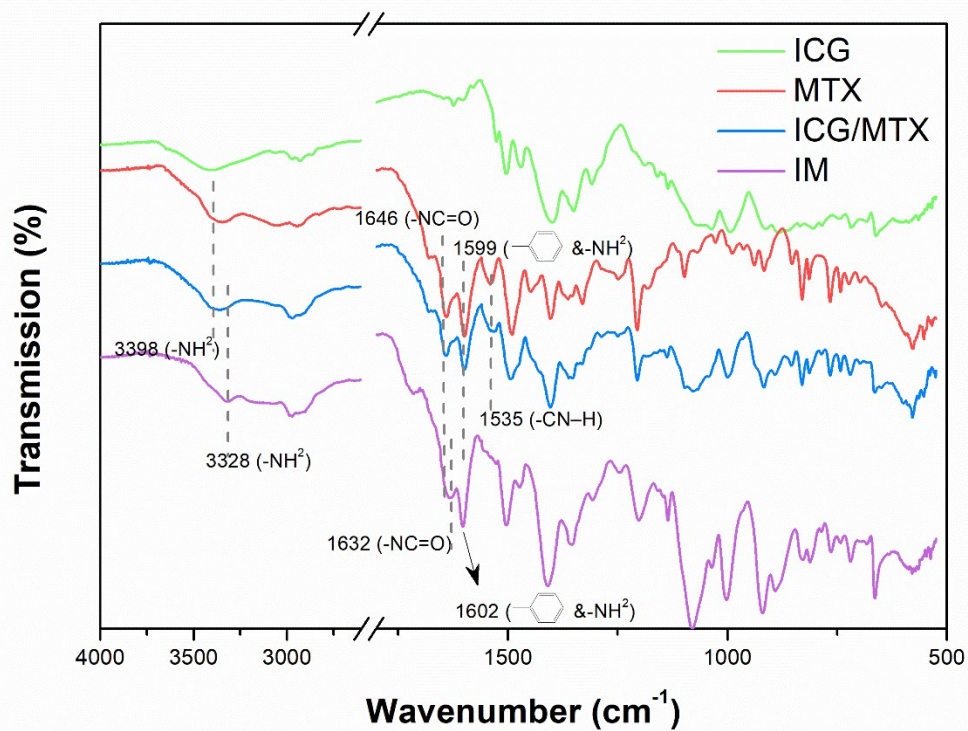
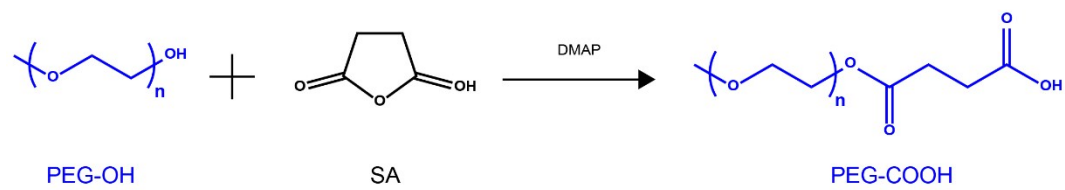


**Fig. S1** FT-IR spectra of ICG, MTX, ICG/MTX mixture, and IM.

Step 1:



Step 2:

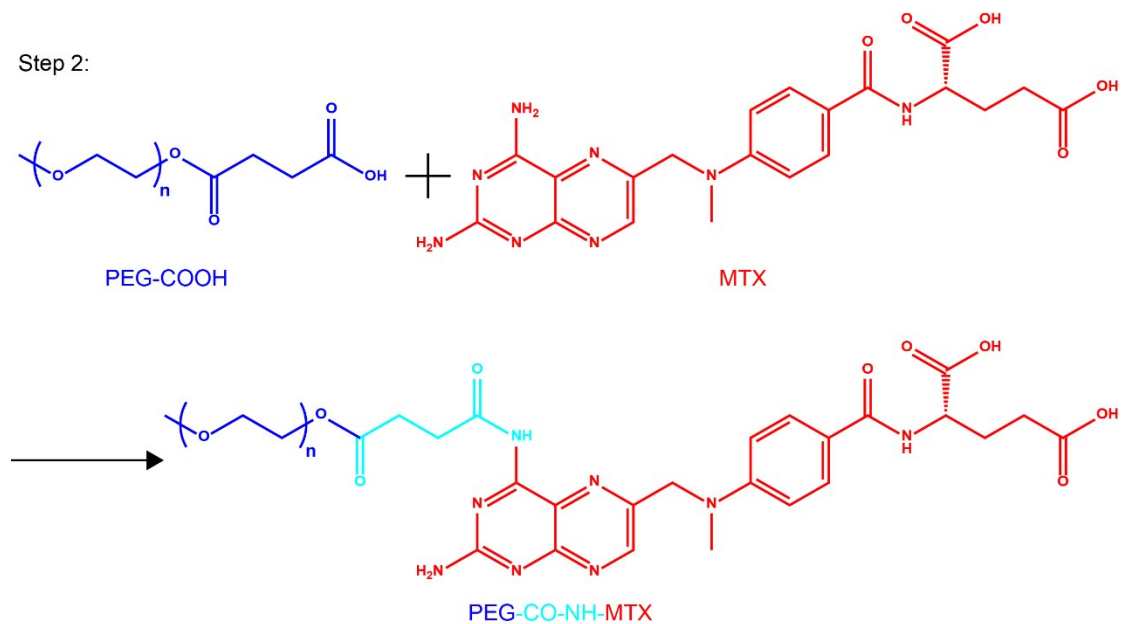


**Fig. S2** Two-step synthesis of acidity-insensitive polymer prodrug PEG-CO-NH-MTX (PEG- MTX).

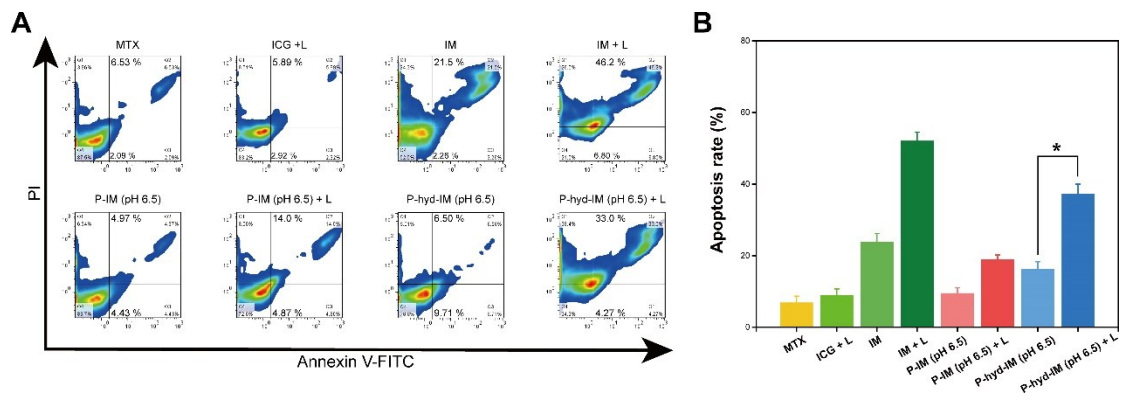


**Fig. S3 (A, B)** Apoptosis analysis of HeLa cells after incubation with ICG, MTX, IM, dePEGylated P-IM, and dePEGylated P-hyd-IM without/with laser irradiation treatment for 12 h incubation. \* $P < 0.05$ .

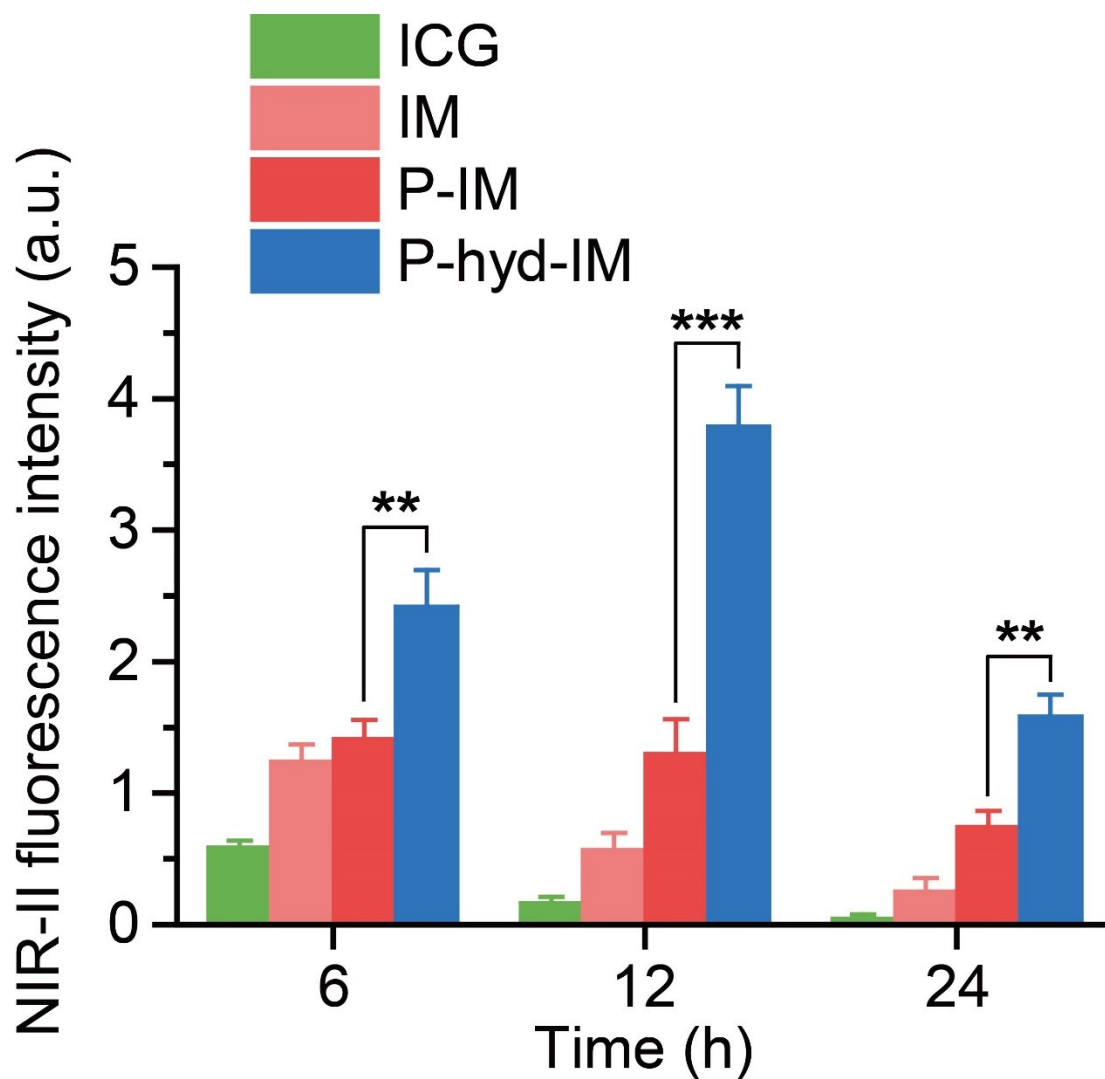


Fig. S4 NIR-II fluorescence intensity in tumors of HeLa tumor-bearing nude mice after *i. v.* injection of ICG, IM, P-IM, and P-hyd-IM. \*\* $P < 0.01$ ; \*\*\* $P < 0.005$ .

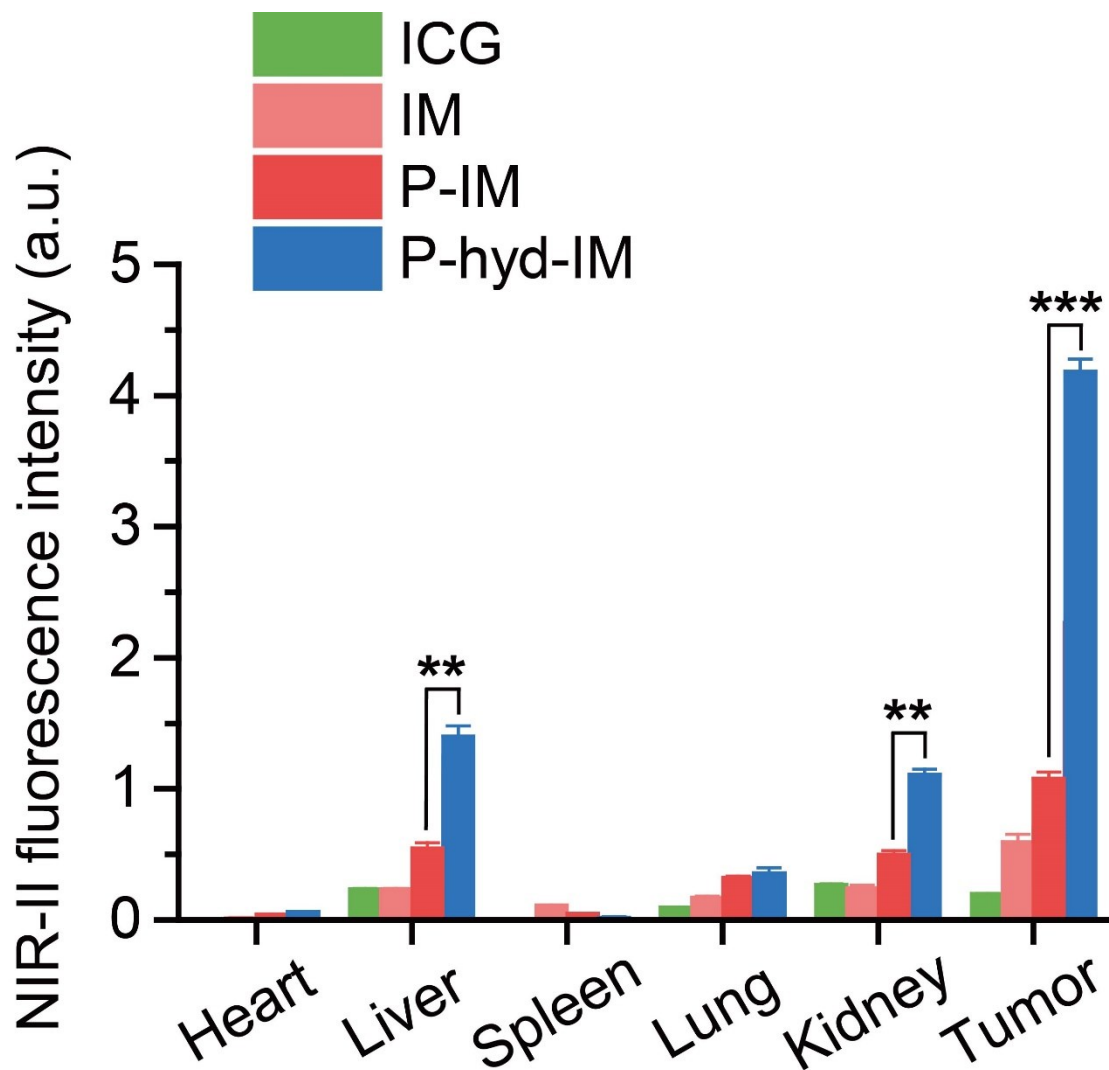
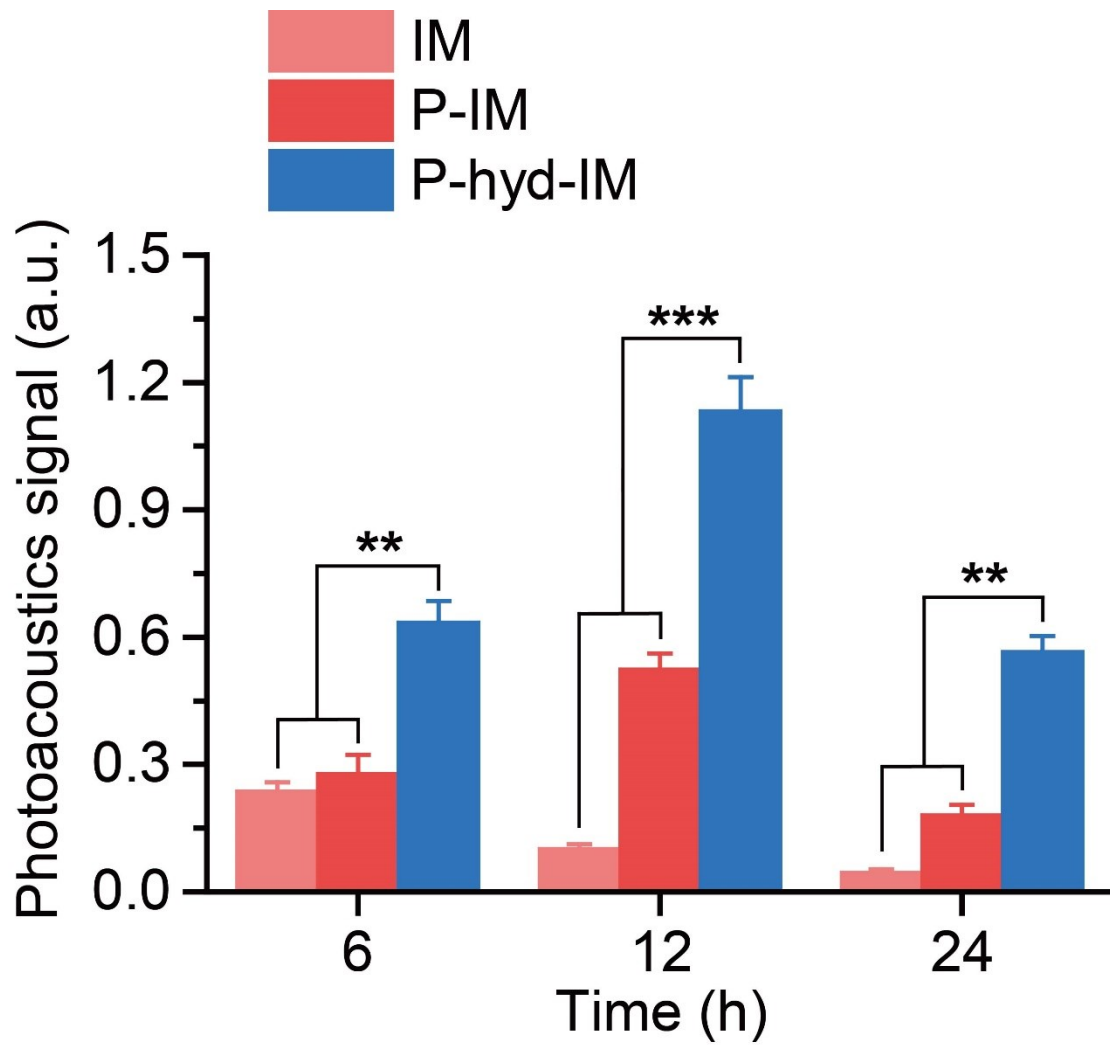
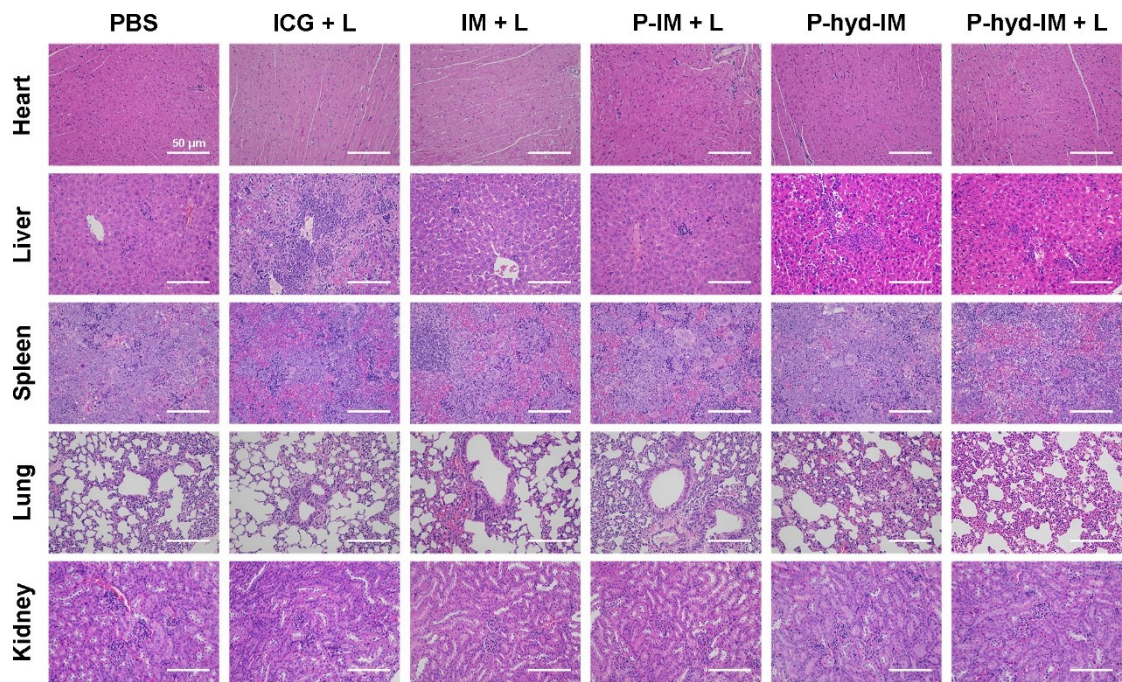


Fig. S5 NIR-II fluorescence intensity of major organs and tumors of ICG, IM, P-IM, and P-hyd-IM at 24 h.  $**P < 0.01$ ;  $***P < 0.005$ .



**Fig. S6** PA intensity of tumors in HeLa tumor-bearing nude mice after *i. v.* injection of ICG-MTX and CA@ICG-MTX. \*\* $P < 0.01$ ; \*\*\* $P < 0.005$ .



**Fig. S7** H&E staining histological images of different groups obtained from tissues including heart, liver, spleen, lung, and kidney of HeLa tumor-bearing mice.